Hubbard model for intermediate-dimensional excitons

Garnett W. Bryant
Optical Processing Branch, U.S. Army Research Laboratory, Adelphi, Maryland, 20783-1197
(Received 7 March 1994)

A Hubbard model is solved exactly to characterize confined, intermediate-dimensional excitons for the full range of electron and hole hopping and interaction strengths. Finite systems with periodic boundary conditions model unconfined excitons. Finite systems with terminated ends model confined excitons. Exciton energies, oscillator strengths, and electron and hole distributions are determined. Oscillator strengths and electron-hole distributions of confined intermediate-dimensional excitons exhibit anomalous, nonmonotonic, nonuniversal dependences on the electron-hole interaction strength and hopping that are counter to the conventional behavior for quantum-confined excitons and free excitons. Perturbation theory is used to clarify the weak and large interaction limits. In the large-interaction limit, an exciton dead layer occurs near the boundary of the system because electron-hole correlation is suppressed near the boundary. Second-order perturbation theory determines the surface potential barrier caused by the suppression of pair correlation near the surface and determines the hopping rate for tunneling into this barrier. In the weak-interaction limit, on-site correlation of a confined electron-hole pair is suppressed by asymmetry in the electron and hole hopping. For large asymmetry in the electron and hole hopping, the oscillation strength of the confined intermediate-dimensional exciton can be less than the oscillator strength of an uncorrelated, noninteracting pair.

I. INTRODUCTION

Excitons in confined systems have been studied intensively in recent years.[1] In the limit of *complete* quantum confinement, the splitting between confined single-particle levels is so large that the electron and hole occupy definite *independent* single-particle states of the confinement potential,[2] and electron-hole correlation in the confined dimensions is quenched. In the bulk limit, the exciton has free center-of-mass motion, determined by the exciton total mass, and internal excitations, determined by the pair reduced mass. The center-of-mass motion is separable from the internal excitations. A simple understanding is possible in each of these limits because the exciton behaves as a composite of two *independent* particles: the electron and hole for the quantum-confined exciton and the free center-of-mass particle and the bound reduced-mass particle for the unconfined, bulk exciton. Neither simple picture provides a good understanding of excitons confined in systems, such as thin films,[3] wide quantum wells and superlattices,[4] microfabricated quantum wires and dots,[5,6] large nanocrystallites and clusters,[7,8] and long chain polymers,[9] which are neither bulk nor quantum-confined systems. In these intermediate-dimensional systems, confinement strongly couples the center-of-mass and relative motion, correlation strongly couples the electron and hole motion, and the intermediate-dimensional exciton is a composite of two *strongly coupled* particles.

Progress toward understanding confined intermediate-dimensional excitons has been made by use of variational calculations[2,8-18] and configuration-interaction calculations.[19-22] Specially constructed variational wave functions have been used to study specific effects, such as electron-hole asymmetry[8,15-17] and the formation of exciton dead layers near the boundary of the system.[18,23] However, no variational wave function has been developed that can model the full range of exciton states. Excitons confined in dots and clusters can be studied by use of configuration-interaction approaches because these systems have discrete energy spectra. Configuration-interaction calculations are numerically exact if enough configurations can be used. However, these calculations are numerically intensive and have only been done for specific systems.

In this paper, I use a Hubbard model to study excitons in confined systems. This simple model is used for three reasons: (1) the exciton states can be determined exactly by numerical diagonalization of this model; (2) one model can be used to represent many qualitatively different confined systems, such as quantum dots, wide quantum wells, superlattices, and polymers; and (3) the same model can be used for the full range of electron and hole hopping and interaction strengths needed to *completely* characterize exciton states in confined systems. As a result, a complete and consistent qualitative understanding of the effects of correlation and quantum-confinement on intermediate-dimensional exciton states can be obtained from one model. This has not yet been achieved by use of variational calculations or configuration-interaction calculations.

The properties of free excitons exhibit universal behavior since the properties do not separately depend on the electron mass, the hole mass, or the electron-hole interaction strength $U(U\sim 1/\varepsilon$, where ε is the bulk dielectric constant). Energies vary as μU^2, and properties that depend on the exciton wave function, such as oscillator strengths and pair distribution functions, vary as μU. The interaction strength U and the reduced mass μ cannot be determined separately unless both energy levels

0163-1829/94/49(23)/16129(12)/$06.00

and wave-function properties are known. The electron and hole masses cannot be determined separately unless the exciton center-of-mass motion, which depends on the exciton total mass, is also probed. The properties of free excitons vary monotonically with μU. Binding energies, electron-hole correlations, and oscillator strengths increase as the interaction strength or the reduced mass is increased.

Intermediate-dimensional excitons exhibit nonmonotonic, nonuniversal dependences on electron and hole masses (hopping rates in the Hubbard model) and interaction strengths, arising from the interplay of confinement and correlation, that are not exhibited by free excitons. The properties of intermediate-dimensional excitons depend separately on the interaction strength, the electron hopping, and the hole hopping because the confinement strongly couples the center-of-mass motion to the reduced-mass motion. This insight is key for developing accurate models of excitons in real confined systems. A Hubbard model for an interacting electron-hole pair in a finite system (a lattice with a finite number of sites) is solved in this paper to exhibit, identify, and clarify this nonmonotonic nonuniversal behavior. To correctly identify this nonuniversal behavior, it is important that one model, which can be applied to the entire range of electron and hole hopping and interaction strengths, be used. If different models were used to study different parameter ranges, then it would not be clear when the nonuniversal nonmonotonic behavior is real and when it arises from differences in the models.

The Hubbard model, described in Sec. II, is solved exactly by numerical diagonalization for finite systems. Three special cases are considered. For systems with periodic boundary conditions, the Hubbard model is transformed from a site representation to a momentum representation. In this representation, it becomes clear that the ground-state exciton in a periodic system exhibits the same universal behavior as a free exciton. Results are obtained for finite systems with periodic boundary conditions and with terminated ends to distinguish the universal and monotonic behavior of free excitons from the nonuniversal nonmonotonic behavior of confined intermediate-dimensional excitons. To clarify this behavior, I use second-order perturbation theory to analyze the weak and large interaction limits.

Results for energies, oscillator strengths, and electron and hole distributions for periodic and confined systems are presented in Sec. III to show how the nonuniversal nonmonotonic behavior of intermediate-dimensional excitons arises. The *energies* of intermediate-dimensional excitons depend monotonically on hopping and interaction strengths just as do the energies for (free) excitons in periodic (bulk) systems. This paper focuses on properties such as oscillator strengths and distribution functions that are determined directly from the exciton wave function and clearly exhibit the nonuniversal nonmonotonic behavior for intermediate-dimensional excitons. The following picture arises from these results (see Fig. 1 for the behavior of an exciton in a confined two-dimensional system). Two possibilities occur depending on whether the electron and hole have similar masses (in the context of the Hubbard model to be defined in Sec. II, if the electron and hole have similar nearest-neighbor hopping rates $T_h \approx T_e$) or the electron and hole have very different masses (there is a large asymmetry in the hopping rates $T_h \ll T_e$). In the limit of weak interaction (the quantum-confinement limit with $U \ll T_h, T_e$), the electron and hole occupy the uncorrelated single-particle states defined by the confining potential. As the electron-hole interaction increases, the electron and hole contract in the potential defined by the distribution of the other particle. If the electron and hole masses are similar, the electron and hole contract similarly as U increases and the pair becomes strongly correlated with the exciton center of mass confined by the boundary of the system. If the masses are very different, then the heavier particle contracts more than the lighter particle and the electron-hole overlap can be reduced by the asymmetry in the electron and hole distributions, even as their motion becomes more strongly correlated. In the limit of very large electron-hole interaction, the exciton moves freely inside a confined system with dead layers near the boundaries. The dead layer arises because the exciton cannot fully correlate near a surface. The effect of this dead layer is determined by how strongly the exciton can tunnel into the layer. Conclusions are presented in Sec. IV.

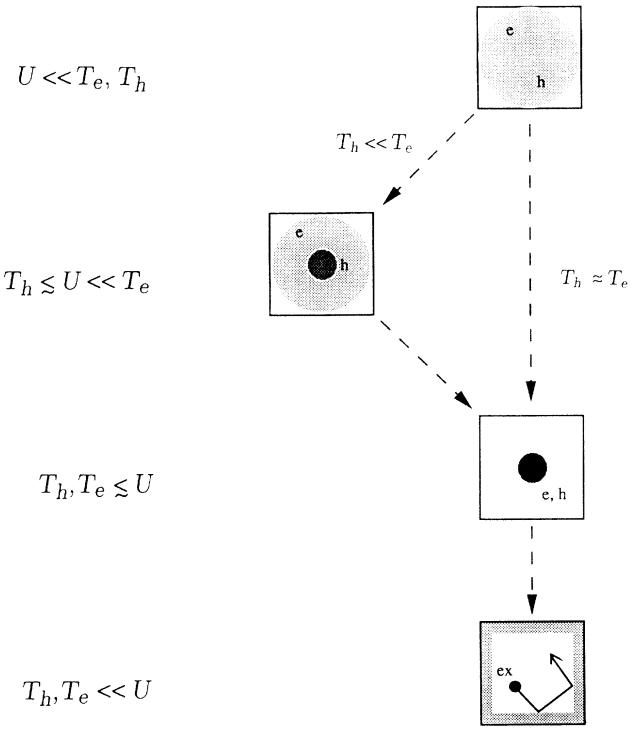

FIG 1. Physical picture for confined intermediate-dimensional excitons.

II. THE HUBBARD MODEL FOR INTERMEDIATE-DIMENSIONAL EXCITONS

Hubbard models are often used to describe interacting many-electron systems on a lattice of sites. Typically, a one-band model is used to describe the hopping and the

electrons partially fill the band. In these models, holes occur as unoccupied states below the Fermi level of the band. The bound excited-electron–hole pairs are determined by taking into account all other electrons.[24] To model a semiconductor, a two-band model must be used. The conduction band contains a few electrons; the valence band contains a few holes. The appropriate Hubbard-like model is a two-component model with only a few particles in each component. In this paper I consider confined intermediate-dimensional systems with one electron-hole pair. The Hubbard Hamiltonian I use to model a single exciton is

$$H=\sum_{i,j}^{N}(T_e c_i^* c_j+T_h d_i^* d_j)+\sum_{i}^{N} U c_i^* c_i d_i^* d_i + \sum_{i,j=\mathrm{NN}}^{N} U_{\mathrm{NN}} c_i^* c_i d_j^* d_j \ . \tag{1}$$

The system has N sites. Here *site* is used loosely. A site could be a well or dot in a superlattice of wells or dots,[4,14] an atomic site in a polymer chain, or a fictitious site defined by a local basis used to represent states in a dot or nanocrystallite. Only nearest-neighbor electron (hole) hopping $T_e(T_h)$, is included. The electron (hole) creation operator at site i is c_i^* (d_i^*). The on-site electron-hole interaction is U. I consider longer-range electron-hole interactions by including a nearest-neighbor interaction with strength U_{NN}. A simple interaction is used so that the model can provide qualitative insight that is common to many different confined systems. For most of the results presented in this paper, only the on-site interaction is included. The results are qualitatively the same when nearest-neighbor interaction is included, and the results are qualitatively similar to results obtained for specific systems by use of variational approaches and configuration interaction approaches with the full electron-hole Coulomb interaction. Electron-electron and hole-hole interactions can be included to study multiexciton states.[25] Linear chains and finite, square two-dimensional arrays are considered here. Confined systems are modeled by systems with terminated ends. Systems modeled with periodic boundary conditions are also considered. As shown below, excitons in systems with periodic boundary conditions exhibit the same universal behavior as bulk excitons. One-exciton wave functions and energies are determined by diagonalization of Eq. (1) and by perturbation theory in the appropriate limits. The nonuniversal, nonmonotonic behavior of confined excitons is most clearly revealed by properties that depend on the exciton wave function. To understand this behavior, I determine electron and hole distributions, electron-hole separation, and oscillator strengths for transitions from the no-pair state to lth one-exciton state,

$$O_l=\left|\langle l|\sum_{i}^{N} c_i^* d_i^*|0\rangle\right|^2 . \tag{2}$$

This negative U, attractive Hubbard model has been used extensively to understand many-body states of high-temperature superconductors and one-dimensional organic superconductors. Calculations have been done for finite systems[26–29] using periodic and twisted boundary conditions to model extended systems. Results presented in this paper provide complementary insight about pair correlations in finite systems with terminated boundaries.

Three special cases are treated analytically for additional insight. First, I show that excitons in systems with periodic boundary conditions exhibit universal behavior. For simplicity, I consider an N-site linear chain with periodic boundary conditions (a ring) and with on-site interaction ($U_{\mathrm{NN}}=0$). First, the electron site operators are transformed to a plane-wave basis by use of transformation

$$c_j^*=\frac{1}{\sqrt{N}}\sum_{k} e^{ikj} c_k^* \ , \tag{3}$$

where the sum is over $k=k_m=2\pi m/N$, for $m=1,2,\ldots,N$. A similar transformation is used for the hole site operators. Equation (1), for a system with periodic boundary conditions, is rewritten in the electron and hole plane-wave basis

$$H=2\sum_{k}\cos(k)(T_e c_k^* c_k+T_h d_k^* d_k) + \left[\frac{U}{N}\right]\sum_{k_1,k_2,k_3,k_4}\delta_{k_1+k_3,k_2+k_4} c_{k_1}^* c_{k_2} d_{k_3}^* d_{k_4} \ . \tag{4}$$

The hopping terms conserve the single-particle momenta. The interaction conserves the pair state total momentum ($K=k_e+k_h$). Thus the pair eigenstates of Eq. (4) must have definite total momentum. The site operator that determines the oscillator strength can also be rewritten in the plane wave basis, $\sum_i^N c_i^* d_i^*=\sum_k c_k^* d_{-k}^*$. Just as in the bulk case, only $K=0$ pair states contribute to the oscillator strength. The $K=0$ Hamiltonian is

$$H_{K=0}=\sum_{k}2(T_e+T_h)\cos(k)\alpha_k^*\alpha_k+\sum_{k_1,k_2}(U/N)\alpha_{k_1}^*\alpha_{k_2} \ , \tag{5}$$

where $\alpha_k=d_{-k}c_k$ is the annihilation operator for a pair with $k_e=-k_h=k$. The properties of the $K=0$ exciton in a ring scale with $U/(T_e+T_h)$. For a bulk exciton, T_e+T_h is proportional to the exciton inverse reduced mass, so the $K=0$ ring exciton has the same scaling properties as a bulk exciton.

The behavior of intermediate-dimensional excitons can be determined in the limits of weak and strong interaction by the use of second-order perturbation theory. First consider the weak interaction limit. For simplicity, consider an N-site linear chain with only on-site interaction. Write

$$H=H_0+V \ , \tag{6a}$$

where the nearest-neighbor hopping Hamiltonian is

$$H_0=\sum_{i,j}^{N} T_e c_i^* c_j+\sum_{i,j}^{N} T_h d_i^* d_j \tag{6b}$$

and

$$V=U\sum_{i}^{N} c_i^* c_i d_i^* d_i \ . \tag{6c}$$

The eigenfunctions of H_0 form the basis for perturbation theory. Let $\phi_n(i)$ be the eigenfunction at site i for the nth eigenstate ($n=1,2,\ldots,N$) with eigenvalue e_n of the single-particle hopping Hamiltonian $H_{\rm SP}=\sum_{i,j}^{N} c_i^* c_j$. The pair eigenstates of H_0 are [$n=(n_e,n_h)$ is the index for the electron and hole single-particle hopping eigenstates]

$$\psi_n^0(i_e,i_h)=\phi_{n_e}(i_e)\phi_{n_h}(i_h) \ , \tag{7}$$

and the energies are $E_n^0=T_e e_{n_e}+T_h e_{n_h}$.

Consider the exciton ground state. The unperturbed ground state is $\psi_g^0(i_e,i_h)=\phi_1(i_e)\phi_1(i_h)$ with energy $E_g^0=(T_e+T_h)e_1$. To second order in perturbation theory

$$\psi_g=\psi_g^0+\psi_g^1+\psi_g^2 \ , \tag{8a}$$

where

$$\psi_g^1=\sum_{n\neq g}\psi_n^0\frac{\langle n|V|g\rangle}{(E_g^0-E_n^0)} \tag{8b}$$

and

$$\psi_g^2=\sum_{n\neq g}\frac{\psi_n^0}{(E_g^0-E_n^0)}\left[\sum_{m\neq g}\frac{\langle n|V|m\rangle\langle m|V|g\rangle}{(E_g^0-E_m^0)}-\frac{\langle g|V|g\rangle\langle n|V|g\rangle}{(E_g^0-E_n^0)}\right]-\frac{1}{2}\langle\psi_g^1|\psi_g^1\rangle\psi_g^0 \ . \tag{8c}$$

The sums include all unperturbed pair states except the ground state. The first term gives the second-order mixing of the unperturbed excited states. The last term arises from the (second-order) change in the wave-function normalization due to the first-order change in the wave function. This term is critical for correctly determining oscillator strengths.

Recall that

$$O_g=\left|\sum_{i=1}^{N}\psi_g(i,i)\right|^2 \ ,$$

where the sum extends over all sites i. Writing $O_g=|A_0+A_1+A_2|^2$, then

$$A_0=\sum_{i=1}^{N}\psi_g^0(i,i)=1 \ , \tag{9}$$

$$A_1=\sum_{i=1}^{N}\sum_{n\neq g}\phi_{n_e}(i)\phi_{n_h}(i)\frac{\langle n_e,n_h|V|1,1\rangle}{(E_g^0-E_{n_e,n_h}^0)} \ ,$$

$$=\sum_{n\neq g}\delta_{n_e,n_h}\frac{\langle n_e,n_h|V|1,1\rangle}{(E_g^0-E_{n_e,n_h}^0)} \ , \tag{10}$$

(the wave functions are taken to be real)

$$=\frac{U}{(T_e+T_h)}\sum_{n>1}\sum_{i=1}^{N}\frac{\phi_n^2(i)\phi_1^2(i)}{(e_1-e_n)} \ ,$$

and

$$A_2=A_{2M}+A_{2N} \ , \tag{11a}$$

where the contribution from second-order mixing is

$$A_{2M}=\sum_{n>1}\frac{U^2}{(T_e+T_h)(e_1-e_n)}\left\{\sum_{m\neq g}\sum_{j,k=1}^{N}\frac{\phi_n^2(j)\phi_{m_e}(j)\phi_{m_h}(j)\phi_{m_e}(k)\phi_{m_h}(k)\phi_1^2(k)}{[T_e(e_1-e_{m_e})+T_h(e_1-e_{m_h})]}\right\}$$
$$-\sum_{n>1}\left\{\frac{U^2\sum_{j=1}^{N}\phi_1^4(j)\sum_{k=1}^{N}\phi_n^2(k)\phi_1^2(k)}{(T_e+T_h)^2(e_1-e_n)^2}\right\} \tag{11b}$$

and the contribution from the second-order change in the normalization is

$$A_{2N}=-\frac{1}{2}U^2\sum_{n\neq g}\frac{\left|\sum_{j=1}^{N}\phi_{n_e}(j)\phi_{n_h}(j)\phi_1^2(j)\right|^2}{[T_e(e_1-e_{n_e})+T_h(e_1-e_{n_h})]^2} \ . \tag{11c}$$

Since $A_1>0$ for an attractive electron-hole interaction, O_g increases for increasing interaction strength in first-order perturbation theory. The correlation induced by the interaction increases the oscillator strength to first order. The sign of A_2 depends on the relative contributions of A_{2M} and A_{2N}. The second-order change in the wave-function normalization gives a negative contribution that decreases O_g. As I will show in Sec. III, nonmonotonic variations in the oscillator strength occur when the asymmetry between the electron and hole is large so that the contribution from the wave-function renormalization becomes important.

To understand the large interaction limit, again consider an N-site linear chain with on-site interaction. For the large U limit, write

$$H=H_0+V \ , \tag{12a}$$

where

$$H_0=U\sum_{i}^{N} c_i^* c_i d_i^* d_i \ , \tag{12b}$$

and

$$V=\sum_{i,j}^{N} T_e c_i^* c_j+\sum_{i,j}^{N} T_h d_i^* d_j \ . \tag{12c}$$

The eigenstates of H_0 are the states $|i,j\rangle$ with the electron at site i and the hole at site j with energy $E_{ij}=U\delta_{ij}$. For $U<0$, the ground state is N-fold degenerate (the states $|i,i\rangle$ with energy U). The degeneracy is preserved in first-order degenerate perturbation theory because first-order hopping does not couple the $|i,i\rangle$ ($\langle i,i|V|j,j\rangle=0$ for all i,j). Second-order perturbation breaks the degeneracy. The eigenstates of H are found to second order in the hopping by diagonalizing

$$H_{ij}^{(2)}=\sum_{k,l=1}^{N}\frac{\langle i,i|V|k,l\rangle\langle k,l|V|j,j\rangle}{E_{ii}-E_{kl}} \ . \tag{13}$$

For nearest-neighbor hopping, the matrix elements vanish unless $|k-l|=1$. Thus, $E_{kl}=0$ for terms that contribute and

$$H_{ij}^{(2)}=\frac{\langle i,i|V^2|j,j\rangle}{U} \ . \tag{14}$$

For $|i-j|>1$, $H_{ij}^{(2)}=0$. For $|i-j|=1$, $H_{ij}^{(2)}=2T_eT_h/U$, since there are two ways for the pair to sequentially hop between adjacent sites. For i not at the end of the chain, $H_{ii}^{(2)}=2(T_e^2+T_h^2)/U$. For i at the end of a terminated chain, $H_{ii}^{(2)}=(T_e^2+T_h^2)/U$. The end sites $i=1, N$ have an energy barrier of height $-(T_e^2+T_h^2)/U$ relative to the interior sites on the chain because the electron and hole can hop in only one direction away from end sites. The correlation energy that the pair can gain by hopping is reduced at the end of the chain. As I will show in Sec. III, this barrier creates a dead layer for the exciton at the ends of the chain.

III. RESULTS

To characterize the effects of confinement and electron-hole interaction on intermediate-dimensional excitons, I consider terminated chains, rings, and finite square two-dimensional arrays. In this paper, I focus on results obtained for terminated chain and rings. Results for two-dimensional arrays are qualitatively similar. First, I discuss the energies, oscillator strengths, and charge distributions for the one-exciton ground-states of 10-site chains and rings. Results are presented for equal electron and hole hopping ($T_h/T_e=1$), intermediate asymmetry in the electron and hole hopping ($T_h/T_e=0.1$) and large asymmetry in the electron and hole hopping ($T_h/T_e=0.001$). Results are presented as a function of U/T_e for $U_{NN}=0$ to show the transition from noninteracting, independent-particle pair states ($U/T_e=0$) to strongly correlated Frenkel-like excitons ($|U/T_e|\gg 1$). Then I discuss how these results change for different chain lengths. The effect of nearest-neighbor interaction is presented to show that including a longer-range interaction does not change the results qualitatively. Finally I discuss the one-exciton excited states of 10-site chains and rings.

Exciton ground-state energies E for 10-site terminated chains with on-site interaction [$U_{NN}=0$] are shown in Fig. 2 (the energy is shifted by the pair interaction U). Exciton ground-state energies for rings are nearly identical to the energies shown for terminated chains. $|E|$ increases monotonically as $|U|$ increases. In Fig. 2, U has been subtracted from the ground-state energy to show the residual pair correlation energy due to the hopping. The correlation energy gained by hopping decreases monotonically as the interaction strength increases and as the hole hopping decreases. When the ground-state energy is scaled by $1/(T_e+T_h)$, rather than $1/T_e$, and plotted as a function of $U/(T_e+T_h)$, rather than U/T_e, the energies for $T_h/T_e=1$, 0.1, and 0.001 lie on the same curve. The universal behavior exhibited by the ground-state energy of the confined exciton is the universal behavior expected for the ground-state energy of an exciton on a ring and for unconfined excitons (see Sec. II). Confined-exciton states are often found through variational approaches to solve the Schrödinger equation that determine the ground-state wave function by minimizing the ground-state energy. Variational wave functions should be chosen carefully since the ground-state energy is not always sensitive to the qualitative differences between terminated chains and rings.

To identify the *qualitative* differences between excitons on rings and excitons on terminated chains, one must consider properties that depend directly on the exciton wave function, such as the oscillator strengths and the charge distributions. Exciton ground-state oscillator strengths O_{EX} for terminated chains and rings [$U_{NN}=0$] are shown in Fig. 3. For rings, O_{EX} increases monotonically as $|U/T_e|$ increases and as T_h/T_e decreases. For $U=0$ (see Fig. 4), $O_{EX}=1$, as expected for a noninteracting-pair state. For large interaction, $O_{EX}=N$ in rings, as expected for a tightly bound electron-hole pair with equal amplitude for being at each site. The three curves for rings shown in Fig. 3 become the same universal curve when they are plotted as a function of $U/(T_e+T_h)$.

O_{EX} for terminated chains is *qualitatively* different from O_{EX} in rings. For terminated chains, O_{EX} is a *nonmonotonic* and *nonuniversal* function of U, T_h, and T_e.

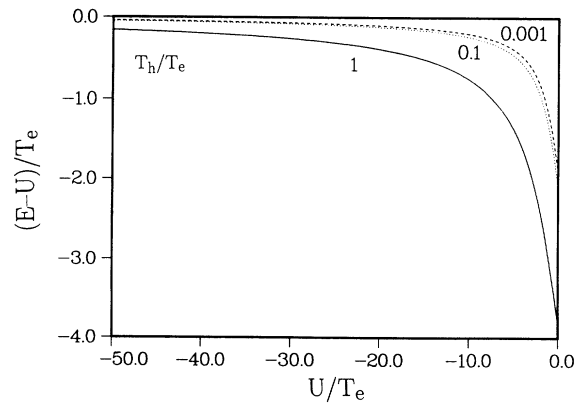

FIG. 2. Exciton ground-state energy for 10-site terminated chains. $T_h/T_e=1$ (solid curve), 0.1 (dotted curve), and 0.001 (dashed curve). The energy is shifted by the pair interaction U.

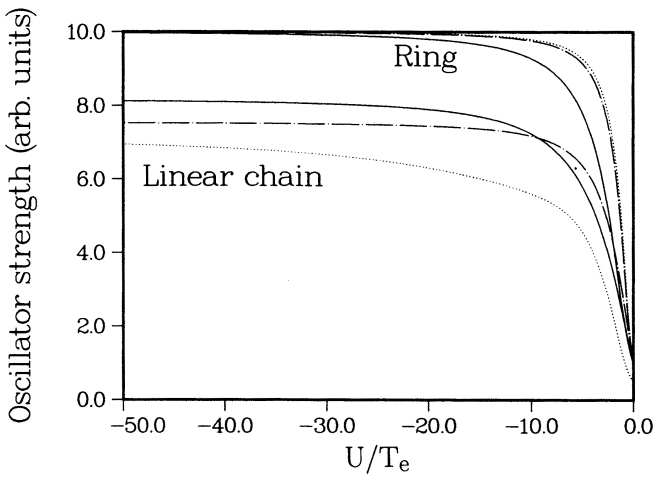

FIG. 3. Exciton ground-state oscillator strength for chains with terminated ends and rings. $N=10$. $T_h/T_e=1$ (solid curves), 0.1 (dot-dash curves), and 0.001 (dotted curves).

For small U, O_{EX} initially increases as $|U|$ increases from zero for all T_h (this is not visible in Fig. 4 for $T_h<0.01$). For $T_h \approx T_e$, O_{EX} continues increasing monotonically with increasing interaction. For $T_h \ll T_e$, O_{EX} increases, decreases, and then increases with increasing interaction. For small U, the confined-exciton oscillator strength varies *nonmonotonically* with T_h/T_e. For large U, the confined-exciton oscillator strength *decreases* monotonically with decreasing T_h, *opposite* to the behavior in a ring. The large U limit for O_{EX} is significantly less than N for a confined system.

The initial increase of O_{EX} as $|U|$ increases from the noninteracting-pair limit can be understood by the use of first-order perturbation theory for small U [Eq. (10)]. When $U=0$, the exciton ground state is the product of electron and hole single-particle ground states ($n_e=n_h=1$). Interactions mix in higher energy pair states. In first-order perturbation theory, mixing in pair states with $n_e=n_h>1$ enhances O_{EX} ($A_1>0$ for both terminated chains and rings, as shown in Fig. 5). Mixing in pair states with $n_e \neq n_h$ does not contribute to O_{EX} in first-order perturbation theory. In second-order perturbation theory, the normalization of the exciton wave function is modified by all of the pair states that are coupled by the pair interaction, including states with $n_e \neq n_h$ that do not contribute to O_{EX}. The amplitudes for pair states with $n_e=h_h$, which contribute to O_{EX}, are reduced if states with $n_e \neq n_h$, which do not contribute to O_{EX}, are also mixed in by the interaction. For rings, the pair interaction does not strongly couple states with $n_e \neq n_h$ to the noninteracting-pair ground state. Pair states with $n_e=n_h$ are preferentially included, and O_{EX} increases monotonically with increasing interaction ($A_1, A_2>0$, see Fig. 5). For terminated chains, pair states with $n_e=n_h$ are preferentially included when $T_h \approx T_e$. In this case, O_{EX} increases monotonically with increasing interaction. When $T_h<0.2T_e$, pair states with $n_e \neq n_h$ are preferentially included and O_{EX} is reduced by the renormalization of the wave function [$T_e A_2/(|U|A_1)<0$, as shown in Fig. 5]. In this case pair states with the hole in an excited level ($n_h>1$, $n_e=1$) are nearly degenerate with the noninteracting-pair ground state and can strongly mix with the noninteracting-pair ground state without contributing to A_1 or A_{2M}. For $T_h>0.2T_e$, A_{2M} makes the dominant (positive) contribution to A_2. For $T_h<0.2T_e$, A_{2N} makes the dominant (negative) contribution to A_2 for linear chains [see Fig. 5; A_{2N} for rings is small, comparable to A_{2N} for terminated chains when $T_h=T_e$]. This second-order reduction is strong enough for weak hole hopping that O_{EX} decreases for a range of

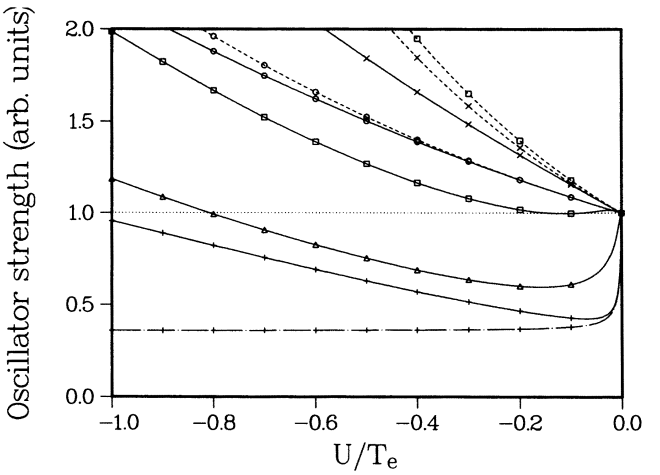

FIG. 4. Exciton ground-state oscillator strength for terminated chains (solid curves) and rings (dashed curves) for weak interaction. $N=10$. $T_h/T_e=1$ (circles), 0.1 (crosses), 0.01 (squares), 0.001 (triangles), and 0.0001 (pluses). The dot-dash curve is the exciton oscillator strength for the electron in its single-particle ground state for $T_h/T_e=0.0001$.

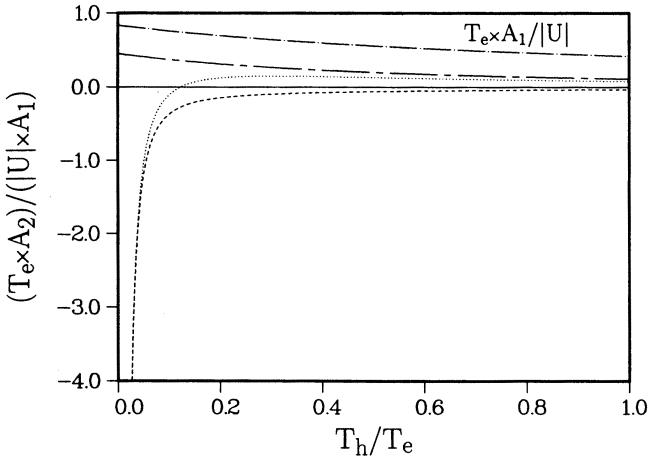

FIG. 5. First- and second-order perturbation contributions to the ground-state oscillator strength for 10-site terminated chains and rings in the weak interaction limit: $T_e A_1/|U|$ for terminated chains and rings (dot-dashed curve), $T_e A_2/(|U|A_1)$ for terminated chains (dotted curve) and rings (long-dash–short-dashed curve), and $T_e A_{2N}/(|U|A_1)$ for terminated chains (dashed curve).

increasing pair interaction and is reduced below the noninteracting-pair limit for 10-site chains. In this range of parameters, interaction suppresses the exciton oscillator strength because the interaction mixes in many configurations that have no oscillator strength. The first-order contribution is dominant until $|U/T_e| = [-|U|A_1/(T_e A_2)]^{1/2}$. Because A_2/A_1 varies as $(1/T_h)^2$ for small T_h [see Eqs. (11b) and (11c) and Fig. 5], the first-order increase in O_{EX} is dominant for a range of U that vanishes as T_h decreases. For weak hole hopping, this initial increase in O_{EX} near the noninteracting-pair limit becomes difficult to see.

One can obtain a physical explanation for the nonmonotonic variation of the oscillator strength in confined systems by considering how the electron and hole localize to form the exciton in confined chains and in rings. First, consider the root-mean-square electron-hole separations in the ground-state exciton of 10-site rings and terminated chains shown in Fig. 6. The pair separation decreases monotonically with increasing interaction and decreasing T_h/T_e. For large interaction, the pair is strongly correlated and the pair separation in the ground-state exciton is the same for rings and terminated chains. For weak interaction, the pair separation is smaller in terminated chains since the confinement forces the pair closer together. In addition, for $T_h \ll T_e$, the pair separation decreases more rapidly with increasing interaction in the weak interaction limit for terminated chains than for rings. These results suggest that the pair is more strongly correlated in a terminated chain than in a ring. One would expect the oscillator strength to be enhanced in terminated chains since the pair separation is less in terminated chains. In fact, trends in exciton properties do not always follow closely the trends in the pair separation. The exciton ground-state energies for rings and chains are nearly the same in the weak interaction limit even though the pair separation for rings and chains are different. For large interaction, the pair separations on rings and terminated chains are the same, but rings have larger pair oscillator strengths. For intermediate and weak interaction, both the pair separation and the oscillator strength are larger on a ring than on a chain.

The electron and hole are distributed uniformly on a ring, so decreasing the electron-hole separation increases the electron-hole on-site correlation uniformly on the ring and increases O_{EX}. Pair distributions in terminated chains are different. To distinguish the effects of confinement, one must consider the electron and hole distributions separately. The electron and hole root-mean-square displacements D from the middle of the terminated chain center are shown in Fig. 7. For weak interaction, the electron (hole) contracts toward the chain center in the attractive potential defined by the hole (electron) distribution. [This self-localization of the intermediate-dimensional exciton explains, for example, the three-dimensional–two-dimensional crossover[4] that occurs for excitons in superlattices of shallow quantum wells as the barrier height is decreased ($|U/T_e|$ and $|U/T_h|$ increase).] On-site correlation at the center of the chain is enhanced, but pair occupation of other sites is suppressed for small $|U|$ and $T_h/T_e \ll 1$ because the hole contracts more than the electron. O_{EX} is suppressed, even though the electron-hole separation is smaller, because fewer sites are occupied. O_{EX} is enhanced at larger $|U|$ because the electron continues to contract while the hole begins to expand to increase on-site correlation away from the chain center.

Exciton states in dots with $T_h \ll T_e$ have been modeled previously by the assumptions that the electron collapses in the potential of a hole fully contracted to the center of the dot[8,16,20] and the hole collapses in the potential of the electron fixed in its lowest-energy single-particle subband.[30] As Figs. 4 and 7 show, the latter model is more appropriate for the smallest $|U|$. O_{EX} calculated for $T_h/T_e = 0.0001$ by use of the latter model is shown in Fig. 4. The model is adequate only for a small

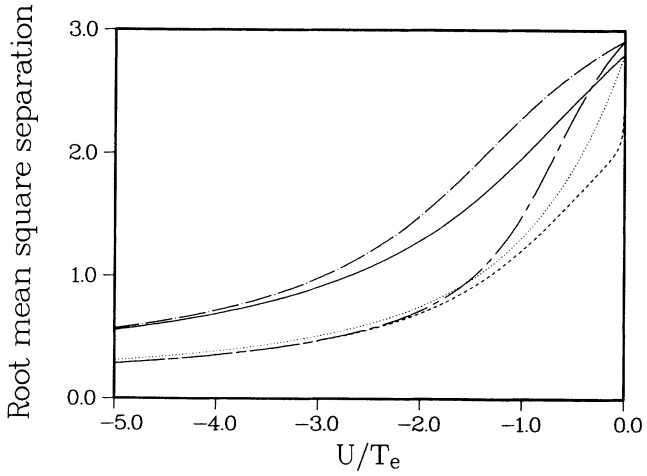

FIG. 6. Root-mean-square electron-hole separation in the ground-state exciton ($N=10$). For a terminated chain: $T_h/T_e=1$ (solid curve), 0.1 (dotted curve), and 0.001 (dashed curve). For a ring: $T_h/T_e=1$ (dash-dot curve), and 0.001 (long-dash–short-dashed curve).

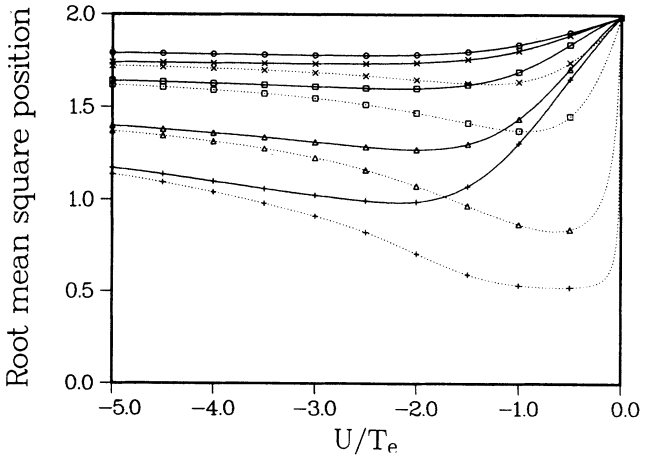

FIG. 7. Root-mean-square displacement of the electron (solid curves) and hole (dotted curves) in the ground-state exciton from the chain center ($N=10$). $T_h/T_e=1$ (circles), 0.3 (×), 0.1 (squares), 0.01 (triangles), and 0.001 (+).

range of $|U|$. The first model becomes more appropriate as the interaction increases.

The electron and hole distributions on a chain expand as the pair interaction increases, becoming nearly equal with the pair tightly bound for large interaction. The exciton center of mass has the same distribution as the electron and hole in the large interaction limit. The electron, hole, and exciton distributions are contracted relative to electron and hole distributions for no interaction, indicating that there is a dead layer[23] at the chain ends where the exciton is excluded. The dead layer can be understood in the large interaction limit by use of the second-order degenerate perturbation theory developed in Sec. II. The pair correlation energy is reduced near a surface, creating a surface potential barrier that repels a tightly bound pair from the chain ends. The pair can still tunnel onto the chain ends because the tightly bound pair can hop, $T_{EX} \equiv H_{ij}^{(2)} = 2T_e T_h / U \neq 0$. Exclusion from the ends becomes complete as T_{EX} (T_e or T_h) decreases. The dead layer increases monotonically with decreasing T_h/T_e. Because of the dead layer, the exciton has fewer sites where it can recombine. O_{EX} is less than N and decreases with decreasing T_h/T_e for large $|U|$ in terminated chains.

The root-mean-square displacement of the quantum-confined single-particle ground state from the center of a one-dimensional, infinite-barrier well with width L is $D_{QC} = L[1/12 - 1/(2\pi^2)]^{1/2} = 0.1808L$. For a single particle in a terminated chain with $N = 10$ (see Fig. 7 for $U = 0$), $D = 1.9876$, so $D/0.1808 = 11$. The 10-site chain has an effective length of 11 units between the positions where the single-particle ground state would vanish if the chain were a quantum well. In the large interaction limit, $D < 1.808$. The effective chain length is no more than 10 units, so the exciton dead region is at least one unit.

The normalized oscillator strength, O_{EX}/N, in a terminated chain, determined by second-order perturbation theory for large $|U|$, is shown in Fig. 8 as a function of N and T_h/T_e. For a tightly bound electron-hole pair with its center of mass confined in a one-dimensional well of length L, $O_{EX}/L = 8/\pi^2$. This limit is shown in Fig. 8. The condition $O_{EX}/N < 8/\pi^2$ provides a criterion for having a dead layer that is different from the criterion that $D < D_{QC}$. The dead-layer criterion based on the oscillator strength is not satisfied for all N or all T_h/T_e. For $T_h/T_e = 1$, $O_{EX}/N > 8/\pi^2$ for all N. For $T_h/T_e < 1$, $O_{EX}/N = 1$ for $N = 2$, decreases as N increases until $O_{EX}/N < 8/\pi^2$, and then monotonically increases, approaching $8/\pi^2$ for large N.

In a quantum well or wire, confinement enhances exciton oscillator strengths because the electron-hole overlap is increased by confinement. For example, the exciton oscillator strength in a narrow quantum well, where the quantum confinement quenches motion across the well, is enhanced by decreasing the well size, because the increased pair binding increases the *lateral* overlap of the pair (in the limit of complete quantum confinement, the pair overlap in the well direction cannot be changed by changing the well size). For intermediate-dimensional excitons, the pair overlap in the confined dimension can be modified by changing the confinement. In that case, as Figs. 4 and 8 show, there is no simple relationship between the degree of confinement and the pair oscillator strength that applies for all N, U, or T_h/T_e.

The nonmonotonic, nonuniversal behavior of intermediate-dimensional excitons on 10-site terminated chains occurs for other chain lengths as well. Ground-state exciton oscillator strengths for rings and terminated chains are shown in Figs. 9–11 as a function of the number of sites N for $T_h/T_e = 1$, 0.1, and 0.001 and for $U/T_e = -50$, -5, and -0.5. The oscillator strength for excitons on rings varies monotonically with T_h/T_e and U/T_e for all N. In the large interaction limit (Fig. 9, $U/T_e = -50$), $O_{EX} = N$ on rings for all N. For intermediate interaction (Fig. 10), O_{EX} increases linearly with N ($O_{EX} \approx \alpha N$) for rings, but full coherence is not achieved

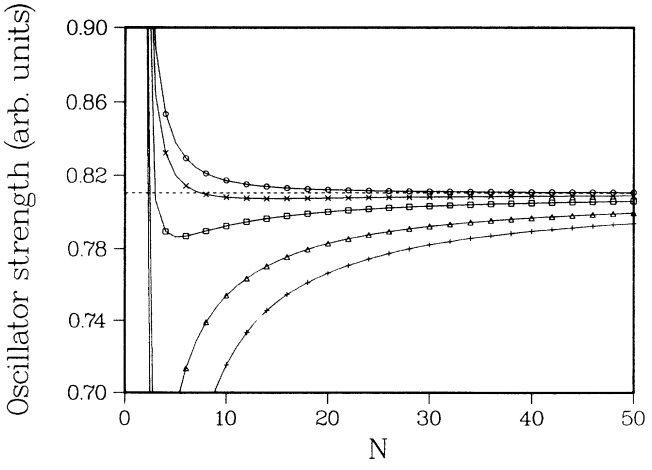

FIG. 8. Normalized ground-state oscillator strength for a chain in the large interaction limit. $T_h/T_e = 1$ (circles), 0.5 (×), 0.3 (squares), 0.1 (triangles), and 0.001 (+). The dashed curve is the large N, large interaction limit. The curves are drawn as a guide.

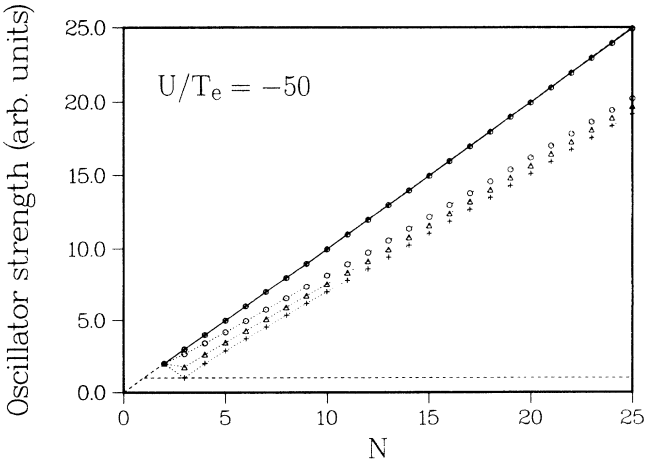

FIG. 9. Exciton ground-state oscillator strength for strong pair interaction ($U/T_e = -50$) on terminated chains (dotted curves) and on rings (solid curves): $T_h/T_e = 1$ (circles), 0.1 (triangles), and 0.001 (+). The dashed lines show the limits $O_{EX} = N$ and $O_{EX} = 1$. The curves are drawn as a guide.

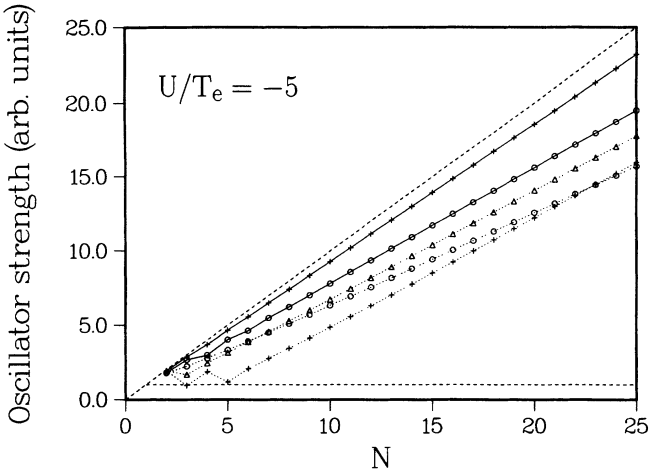

FIG. 10. Exciton ground-state oscillator strength for intermediate pair interaction ($U/T_e=-5$) on terminated chains (dotted curves) and on rings (solid curves): $T_h/T_e=1$ (circles), 0.1 (triangles), and 0.001 (+). The dashed lines show the limits $O_{EX}=N$ and $O_{EX}=1$.

($\alpha<1$). For weak interaction (Fig. 11), O_{EX} shows finite-size effects, increasing monotonically for even N and for odd N with nonmonotonic variations between even and odd N. The magnitude of this finite-size effect decreases as N increases and as the pair correlation increases (U/T_e increases or T_h/T_e decreases). Finite-size effects are smaller for terminated chains, since the pair correlation is stronger on terminated chains. The finite-size effects for rings and terminated chains are out of phase. For terminated chains, O_{EX} is determined by where the hole localizes. For odd (even) N the hole localizes to the one (two) central site(s) of the chain. O_{EX} is greater for even-site chains because the exciton is localized in a larger region. For rings, each site is equivalent,

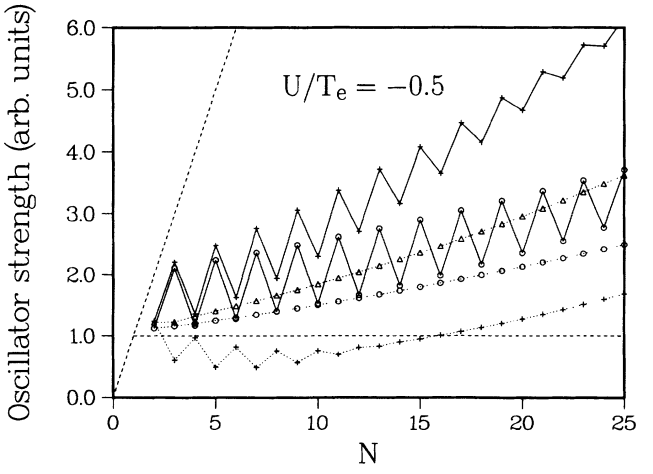

FIG. 11. Exciton ground-state oscillator strength for weak pair interaction ($U/T_e=-0.5$) on terminated chains (dotted curves) and on rings (solid curves): $T_h/T_e=1$ (circles), 0.1 (triangles), and 0.001 (+). The dashed lines show the limits $O_{EX}=N$ and $O_{EX}=1$.

so O_{EX} is determined by how strongly the pair can correlate. For odd (even) N, the hole localizes to the one (two) site(s) nearest the electron. O_{EX} is greater for odd-site rings because the pair overlap is larger.

The same effects of dead layers for strongly interacting pairs and of electron-hole asymmetry for weakly interacting pairs occur for all terminated chains. The dead layer (O_{EX}) increases (decreases) with decreasing hole hopping for all N in the strong interaction limit. The reduction of O_{EX} due to the dead layer is only weakly dependent on the chain length. In the weak interaction limit, O_{EX} is suppressed by the asymmetry in the charge localization for $T_h \ll T_e$ for all chain lengths [$O_{EX}(T_h \ll T_e) < O_{EX}(T_h \approx T_e)$ for all N]. For short chains, O_{EX} is suppressed below the noninteracting pair limit ($O_{EX}=1$) when $T_h \ll T_e$. For longer chains, O_{EX} is still suppressed by the asymmetry when $T_h \ll T_e$, but $O_{EX}>1$ because there are more sites where the pair can recombine. For intermediate pair interaction on terminated chains (Fig. 10), O_{EX} shows a crossover from normal (bulklike) to intermediate-dimensional behavior as the chain length changes that occurs for different N depending on the interaction and hopping. Define the crossover point to be the chain length $N_c(U,T_h)$, where $O_{EX}(U,T_h) = O_{EX}(U,T_h=T_e)$. For large interaction, N_c marks the crossover where dead layer effects become important. For weak interaction, N_c marks the crossover where hopping asymmetry becomes important. For $T_h \approx T_e$, N_c shifts monotonically to shorter chain length as the pair interaction decreases. For $T_h \ll T_e$, the crossover point shifts monotonically to shorter chain length as the pair interaction strength decreases when the pair interaction is large and dead layer effects are important. The crossover point shifts back toward larger chain length as the pair interaction strength becomes weak and the asymmetry effects become important. As a consequence, the exciton on a terminated chain behaves as an intermediate-dimensional exciton for all chain lengths in the large and weak interaction limits and can cross over to bulklike for intermediate interaction strength.

I have obtained the results discussed so far by ignoring nearest-neighbor and longer-range pair interaction. For an electron-hole pair on a polymer chain or in a superlattice of quantum wells or dots (where each well or dot is represented by a site), nearest-neighbor interactions may not be important. For a pair in a single dot (where the sites represent different sites in the same dot) the real pair interaction will be longer range than an on-site interaction. To show how the results presented so far change if a longer-range interaction is included, I have investigated excitons on 10-site terminated chains with a nearest-neighbor pair interaction ($U_{NN}=0.25\,U$). No qualitative change and only small quantitative changes occur when the nearest-neighbor pair interaction is included. O_{EX} calculated with and without U_{NN} are compared in Fig. 12. For large pair interaction, including the nearest-neighbor interaction suppresses O_{EX} because the dead layer is wider for a longer-range potential (the pair is contracted more toward the center of the chain) and because the on-site pair correlation is reduced (for large U) when

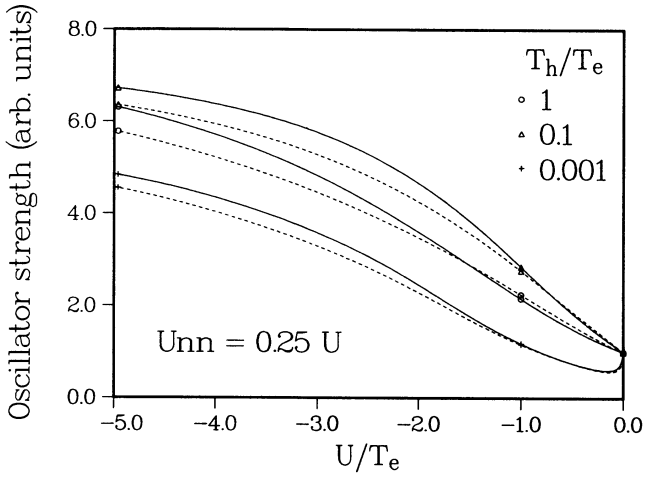

FIG. 12. Exciton ground-state oscillator strength on 10-site terminated chains without nearest-neighbor-pair interaction (solid curves) and with nearest-neighbor-pair interaction $U_{NN}=0.25\ U$ (dashed curves): $T_h/T_e=1$ (circles), 0.1 (triangles), and 0.001 (+).

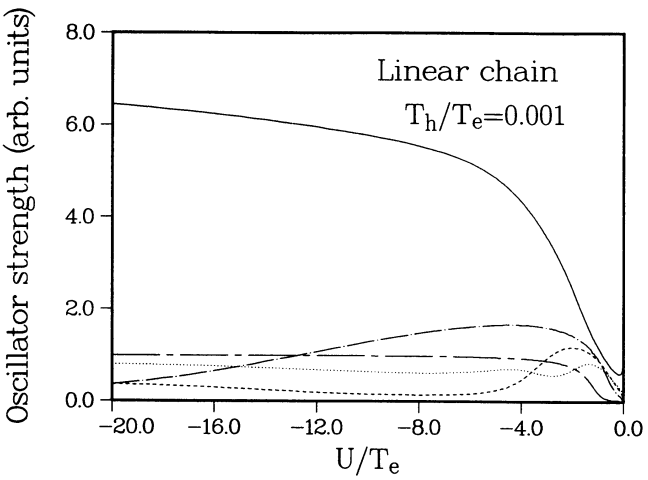

FIG. 14. Oscillator strengths for the 10 lowest-energy pair states (index l) of a 10-site terminated chain, $T_h/T_e=0.001$: $l=1$ (ground state, solid curve), $l=3$ (dotted curve), $l=5$ (dashed curve), $l=7$ (dash dot curve), and $l=9$, 10 (long dash short dash curve). States $l=2$, 4, 6, and 8 are optically inactive.

there is a nearest-neighbor attractive interaction. For weak pair interaction, including the nearest-neighbor interaction enhances the contraction of the electron and hole toward the center of the chain and reduces the pair separation. For $T_h \ll T_e (T_h \approx T_e)$ the oscillator strength is suppressed (enhanced) by this additional contraction. For intermediate pair interaction (the region in Fig. 7 where the electron and hole distributions begin to expand as the pair interaction increases and the pair crosses over from the quantum-confined limit to the tightly bound limit), the pair is less contracted when U_{NN} is included, because U_{NN} reduces the on-site pair correlation of a strongly bound pair.

Excited pair states exhibit the same behavior displayed by the ground state. The excited-state energies vary monotonically with the interaction strength and hopping both for rings and for terminated chains. Excited-state oscillator strengths on rings (see Fig. 13) also vary monotonically with U/T_e and T_h/T_e and follow a universal curve when plotted as a function of $U/(T_e+T_h)$. For terminated chains (see Fig. 14 for the case with large asymmetry in the electron and hole hopping) the excited-state oscillator strengths are nonmonotonic and nonuniversal. The oscillator strength lost by the ground state due to the confinement is shared among several excited pair states. In particular, only the ground state on a ring is optically active in the large interaction limit. On a terminated chain several pair states remain optically active in the large U limit. The excited states (state index $l=9$, 10) with the largest oscillator strength in the large interaction limit are the two states with the pair localized at either end of the chain. These states are trapped in the dead layer but they remain optically active. In the weak interaction limit the first two optically active excited states are the pair state with the electron and hole contracted to the sites next to the middle of the chain (for $l=3$) and the pair state with the electron and hole contracted to the sites second from the middle of the chain (for $l=5$).

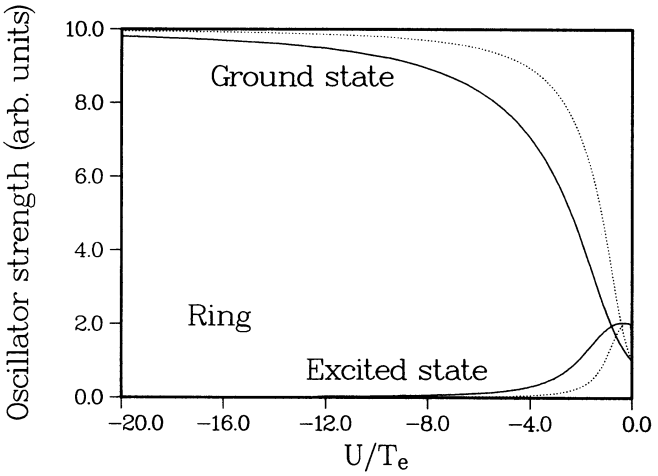

FIG. 13. Oscillator strengths for the 15 lowest-energy pair states of a 10-site ring: $T_h/T_e=1$ (solid curves) and 0.001 (dotted curves). Only one excited state has a finite oscillator strength.

IV. CONCLUSIONS

In summary, a Hubbard model has been solved exactly to characterize intermediate-dimensional excitons for the full range of electron and hole hopping and interaction strengths. The Hubbard model provides an excellent qualitative model for intermediate-dimensional excitons that is generally applicable to a wide variety of systems, including wide quantum wells, quantum dots and microcrystallites, multiple quantum wells, quantum dot arrays, and polymers. However, the model is too simple to be a realistic model for all of these systems.

The intermediate-dimensional exciton is a composite

particle made from two strongly coupled particles: the electron and hole strongly coupled by the pair interaction or the center-of-mass particle and the reduced-mass particle strongly coupled by the confinement. In contrast, the free exciton is a composite particle made from uncoupled center-of-mass and reduced-mass particles, and the quantum-confined exciton is an uncorrelated electron and hole pair. The energy of intermediate-dimensional excitons and bulklike free excitons are qualitatively the same in the Hubbard model. To clearly identify the characteristics of confined excitons, one must consider exciton properties that depend directly on the exciton wave function. Oscillator strengths and electron-hole distributions of intermediate-dimensional excitons exhibit anomalous, nonmonotonic, nonuniversal dependences on the electron-hole interaction strength and hopping that occur due to asymmetry in the electron and hole distributions and to dead layers induced because the interplay of confinement and correlation strongly couples the particles that form the intermediate-dimensional exciton.

For strong pair interaction, the intermediate-dimensional exciton is a tightly bound pair repelled from the boundary of the system because pair correlation is inhibited at the boundary. The exciton ground-state oscillator strength is suppressed because the pair in the ground state cannot recombine in the dead layer at the boundary. For weak pair interaction, the electron and hole each contract in the distribution of the other particle. Large asymmetry in the localization of the electron and hole results when there is a large asymmetry in the electron and hole hopping. The oscillator strength is suppressed in this case because the slowly hopping particle is localized to the middle of the distribution of the other particle, drastically reducing where the pair can recombine. By solving for the full range of interaction strengths and hopping, the transition between these two regimes and the anomalous, nonmonotonic, nonuniversal behavior arising from these effects can be identified. The key qualitative results are independent of the number of sites on the chain and of the inclusion of longer-range pair interactions beyond the on-site pair interaction. Excited states of the intermediate-dimensional excitons exhibit similar anomalous behavior arising from the dead layers and asymmetry in the electron and hole distributions.

Finite-size effects occur in small systems (systems with a few sites in the Hubbard model, i.e., a short chain polymer, a multiple quantum well system with only a few wells, etc.). There are anomalous variations between even-member systems and odd-member systems that can be attributed to the effects of asymmetry in the charge localization of intermediate-dimensional excitons. These finite-size effects could provide a simple, direct signature for excitons in the intermediate-dimensional regime.

ACKNOWLEDGMENTS

Most of this work was performed while the author was a member of the Microphotonic Devices Branch of the Army Research Laboratory.

[1] *Optics of Excitons in Confined Systems*, edited by A. D'Andrea, R. Del Sole, R. Girlanda, and A. Quattropani (The Institute of Physics, Bristol, 1992).
[2] G. W. Bryant, Phys. Rev. B **37**, 8763 (1988).
[3] Z. K. Tang, A. Yanase, T. Yasui, Y. Segawa, and K. Cho, Phys. Rev. Lett. **71**, 1431 (1993).
[4] I. Brener, W. H. Knox, K. W. Goosen, and J. E. Cunningham, Phys. Rev. Lett. **70**, 319 (1993); G. Platero and M. Altarelli, in *Proceedings of the 20th International Conference on the Physics of Semiconductors* (World Scientific, Singapore, 1990), p. 1489, and the references therein to earlier work.
[5] K. Kash, D. D. Mahoney, B. P. Van der Gaag, A. S. Gozdz, J. P. Harbison, and L. T. Florez, J. Vac. Sci. Technol. B **10**, 2030 (1992).
[6] K. Brunner, U. Bockelmann, G. Abstreiter, M. Walther, G. Bohm, G. Trankle, and G. Weimann, Phys. Rev. Lett. **69**, 3216 (1992).
[7] M. G. Bawendi, W. L. Wilson, L. Rothberg, P. J. Carroll, T. M. Jedju, M. L. Steigerwald, and L. E. Brus, Phys. Rev. Lett. **65**, 1623 (1990).
[8] J. Wormer, M. Joppien, G. Zimmerer, and T. Moller, Phys. Rev. Lett. **67**, 2053 (1991).
[9] T. Tokihiro and E. Hanamura, Phys. Rev. Lett. **71**, 1423 (1993).
[10] L. C. Andreani and A. Pasquarello, Phys. Rev. B **42**, 8928 (1990).
[11] Y. Kayanuma, Solid State Commun. **59**, 405 (1986).
[12] T. Takagahara, Phys. Rev. B **36**, 9293 (1987).
[13] T. Takagahara, Phys. Rev. B **47**, 4569 (1993).
[14] G. W. Bryant, Phys. Rev. B. **47**, 1683 (1993).
[15] S. V. Nair, S. Sinha, and K. C. Rustagi, Phys. Rev. B **35**, 4098 (1987).
[16] A. I. Ekimov, Al. L. Efros, M. G. Ivanov, A. A. Onushchenko, and S. K. Shumilov, Solid State Commun. **69**, 565 (1989).
[17] C. F. Lo and R. Sollie, Solid State Commun. **79**, 775 (1991).
[18] A. D'Andrea and R. Del Sole, Solid State Commun. **74**, 1121 (1990).
[19] H. M. Schmidt and H. Weller, Chem. Phys. Lett. **129**, 615 (1986).
[20] Y. Kayanuma, Phys. Rev. B **38**, 9797 (1988).
[21] Y. Z. Hu, M. Lindberg, and S. W. Koch, Phys. Rev. B **42**, 1713 (1990).
[22] V. Halonen, T. Chakraborty, and P. Pietilainen, Phys. Rev. B **45**, 5980 (1992).
[23] J. J. Hopfield and D. G. Thomas, Phys. Rev. **132**, 563 (1963).
[24] See for example, J.-P. Gallinar, Phys. Rev. B **48**, 5013 (1993); D. G. Clarke, *ibid.* **48**, 7520 (1993).
[25] Two-pair states have also been studied by extending the Hamiltonian to include on-site electron-electron and hole-hole repulsion and will be reported elsewhere.
[26] K. Kuroki, H. Aoki, and Y. Takada, J. Phys. Soc. Jpn. **61**, 1161 (1992).

[27]R. M. Fye, M. J. Martins, D. J. Scalapino, J. Wagner, and W. Hanke, Phys. Rev. B **45**, 7311 (1992).
[28]D. Bormann, T. Schneider, and M. Frick, Europhys. Lett. **14**, 101 (1991).
[29]D. Bormann, T. Schneider, and M. Frick, Z. Phys. B: Condens. Matter **87**, 1 (1992).
[30]Al. L. Efros and A. V. Rodina, Solid State Commun. **72**, 645 (1989).

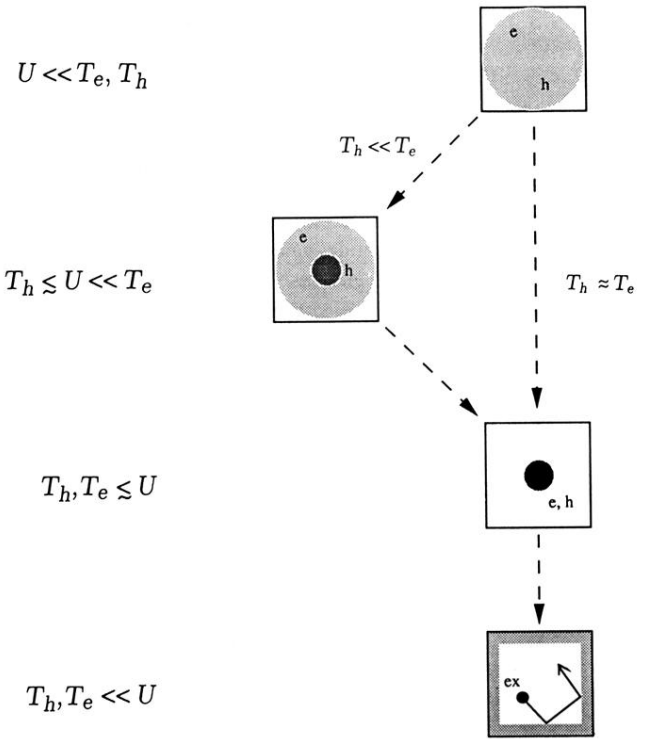

FIG 1. Physical picture for confined intermediate-dimensional excitons.